Arabian Journal of Chemistry (2021) **14**, 103451

King Saud University

Arabian Journal of Chemistry

www.ksu.edu.sa
www.sciencedirect.com

ORIGINAL ARTICLE

Spectrochemical analysis using LIBS and ICP-OES techniques of herbal medicine (*Tinnevelly Senna* leaves) and its anti-cancerous/antibacterial applications

R.K. Aldakheel [a], M.A. Gondal [b,*], M.A. Almessiere [a,c], S. Rehman [d], M.M. Nasr [e], Z. Alsalem [f], F.A. Khan [g,*]

[a] *Department of Physics, College of Science, Imam Abdulrahman Bin Faisal University, Dammam P.O. Box 1982, Saudi Arabia*
[b] *Laser Research Group, Physics Department, IRC Hydrogen – Energy Storage and K. A. Care Energy Research and Innovation Center, King Fahd University of Petroleum & Minerals, Dhahran 31261, Saudi Arabia*
[c] *Department of Biophysics, Institute for Research and Medical Consultations (IRMC), Imam Abdulrahman Bin Faisal University, Dammam P.O. Box 1982, Saudi Arabia*
[d] *Department of Epidemic Diseases Research, Institute for Research & Medical Consultations (IRMC), Imam Abdulrahman Bin Faisal University, Dammam 31441, Saudi Arabia*
[e] *Research Center, Physics Department, Riyadh Elm University, Riyadh 11343, PO. Box 321815, Saudi Arabia*
[f] *Department of Epidemic Diseases Research, Institute for Research & Medical Consultations (IRMC), Imam Abdulrahman Bin Faisal University, Dammam 31441, Saudi Arabia*
[g] *Department of Stem Cell Research, Institute for Research & Medical Consultations (IRMC), Imam Abdulrahman Bin Faisal University, Dammam 31441, Saudi Arabia*

Received 4 July 2021; accepted 19 September 2021
Available online 27 September 2021

KEYWORDS

Senna leaves;
Herbal medicine, nutrients;
Time delay;
Energy;
ICP OES;
CF-LIBS;
Antibacterial;

Abstract *Tinnevelly senna* leaves are being applied to cure many diseases especially in developing countries and sub-Saharan region due to many bioactive compounds such as sennosides, phenols, and flavonoids. The conventional methods to isolate and analyze plant extracts biomolecules are not very effective as well cost effective as they require hazardous chemical solvents and reagents, which are time-consuming processes. The major objective of the present study is to investigate the feasibility of the Laser induced breakdown spectroscopy (LIBS) technique for rapid, eco-friendly, and multi-elemental analysis of *Senna* leaves extracts and study their antibacterial and anticancer potentials. The elegant LIBS technique was applied as a qualitative and quantitative

* Corresponding authors.
E-mail addresses: magondal@kfupm.edu.sa (M.A. Gondal), fakhan@iau.edu.sa (F.A. Khan).
Peer review under responsibility of King Saud University.

Production and hosting by Elsevier

https://doi.org/10.1016/j.arabjc.2021.103451

Scanning electron microscope (SEM);
Anticancer;
Cell metabolic activity MTT assay

method for *Senna* leaves sample's elemental analysis and their biological activities were measured by evaluating anti-cancer and anti-bacterial analysis. The quantitative analysis of *Senna* leaves extracts was done using the calibration-free laser-induced breakdown spectroscopy (CF-LIBS) algorithm showing their appreciable content of several nutrient elements, and the obtained results were in close conformity with these achieved by using the standard analytical ICP OES technique. We studied the bactericidal efficacy of the *Senna* leaves extract against *Staphylococcus aureus* (*S. aureus*) by AWD assays and morphogenesis by scanning electron microscopy (SEM) and the anticancer activity was also investigated where different concentrations of *Senna* leaves extract were tested on cancer cells (HCT-116 and HeLa) and normal cells (HEK-293) using the cell metabolic activity MTT assay and Propidium iodide (PI) staining. We have also calculated the inhibitory concentration (IC50) value for the various extracts concentrations (25 μg/ml, 50 μg/ml, 100 μg/ml, 150 μg/ml, 200 μg/ml, and 225 μg/ml). We have found that IC_{50} value for HCT-116 cells were 13.5 μg/ml, 17.5 μg/ml, 21.5 μg/ml, 22.5 μg/ml, 26 μg/ml and 33.5 μg/ml and for HeLa cells 15.25 μg/ml, 21.25 μg/ml, 23.5 μg/ml, 262.5 μg/ml, 36.25 μg/ml, and 39.50 μg/ml. The bactericidal efficacy of the *Senna* leaves extract showed significant inhibition against Gram-positive bacterium. Both MTT and PI analysis showed that *Senna* leaves extract induced profound inhibition on HCT-116 growth and proliferation. Additionally, *Senna* leaves extract did not exert an inhibitory influence on normal (HEK-293), which is non-cancerous cells. We suggest that the extract specifically targets the cancerous cells, which could be highly beneficial for the development of future safe anticancer and antibacterial drugs using these extracts.

1. Introduction

Cassia Angustifolia Vahl., belonging to the Leguminosae family, is a perennial erect shrub (Hanif et al. 2020), and commercially traded as *Tinnevelly senna* (*Senna*) (Tripathi, 1999). *Senna* is recognized as a traditional medicinal-valuable herb in curing occasional-occurring constipation as its constitutional hydroxyanthracenes components appear to contribute to the purgative properties. The purgative effectiveness of *Senna* is well reported in various worldwide pharmacopeias and monographs (Blumentthal et al., 2000). *Senna* leaves are traditionally used to cure many diseases like liver injury, fevers, jaundice, enlarged spleen, etc (Usmanghani et al., 1997) Various pharmacological properties have been reported for *Senna* leaves, including antidiabetic (Jani and Goswami, 2020; Osman et al., 2017), antioxidant (Ahmed et al., 2016; Ahmed et al., 2018; Farid et al., 2020), anticancer (Ahmed et al., 2016), antimutagenic (Ahmed et al., 2018; Farid et al., 2020; Silva et al., 2008), antimicrobial (Ahmed et al., 2016; VijayaSekhar et al., 2016), hepatoprotective (Bellassoued et al., 2019; Kamaraj et al., 2010; Vitalone et al., 2011), anti-inflammatory (Ahmed et al., 2018; Farid et al., 2020), and insecticidal and larvicidal (Zhu et al., 2020) effects. Different biochemically active compounds (e.g., sennosides, phenols, and flavonoids) contained in the *Senna* leaves are responsible for its pharmacologic benefits as an herbal medicine.

There are numerous atomic spectroscopic techniques for the elemental analysis of various biomaterials, which are flame atomic absorption spectrometry (F AAS), laser ablation inductively coupled plasma mass spectrometry (ICP-MS), and inductively coupled plasma optical emission spectroscopy (ICP OES), respectively. Although these conventional analytical techniques are highly sensitive, they involve lengthy procedures for the sample preparation using hazardous chemical solvents and reagents, are time-consuming, and unsuitable for in-field or remote monitoring (Liu et al., 2015; Tripathi et al., 2015). On the other hand, laser-induced breakdown spectroscopy (LIBS) is based on the optical emission spectrometry, has emerged as a robust alternative analytical spectroscopic method in the field of multi-elemental detection. LIBS has several advantages over the above-mentioned competing analytical techniques for the spectrochemical analysis as it is a safe, very little sample preparation, no reagents or chemicals required and rapid technique. It doesn't involve ashing or wet acid digestion for the sample preparation, providing in-situ or remote and synchronous multiple elemental detections, and applicability for samples of different phases (e.g., solids, liquids, or gases) (Liu et al., 2015; Senesi et al., 2019).

LIBS technique is applied to a wide variety of biomaterials, including plants with their different parts (Andrade et al., 2018, 2017; Rehan et al., 2021; Senesi et al., 2019). There is an increasing curiosity in analyzing the plant leaves elemental content since many leaves of varied species are used as herbal drugs. A recent study demonstrated that the LIBS analysis of the miracle leaves of the medicinal *Moringa oleifera* plant revealed high contents of the nutrients like Ca, K, S, Mg, P, Na, Fe, Mn, Zn, and Cu (Aldakheel et al., 2020a). Similarly, 17 different elements were detected using the LIBS system in both henna dried-leaves and dried soil, such as Ca, Na, Mg, Al, Fe, K, Si, S, P, Mn, Sr, Ba, Zn, Cr, Cu, and Ni (Rehan et al., 2019). The majority of these elements were also observed in LIBS spectra of dried leaves from three traditionally used herbal medicines in Pakistan (Jabbar et al., 2019). *Ocimum* L. species were optically classified, founding the emissions of Ca, K, Mg, Na, H, C, N, and O elements (Tripathi et al., 2015). LIBS technique was successfully applied to discriminate between leaves of the Asian herbal medicine *Blumea balsamifera* DC from two provinces in China relying on spectral lines of five elements K, Na, Ca, Al, and O (Liu et al., 2015).

The elemental composition of one of the *Senna* products, a tea bag of the crude powdered *Senna* leaves, was determined using the conventional analytical techniques ICP OES and

ICP-MS. Several elements were detected including, Al, Ba, Ca, Cu, Fe, Mg, Mn, Na, Sr, Zn, As, and V (Levine et al., 2004). From this point of view, the objective of the present study was aroused to investigate the feasibility of the LIBS technique for rapid, eco-friendly, and reliable qualitative and quantitative multi-elemental analysis of dried and powdered *Senna* leaves. There are elemental analytes of nutritional value, while others of toxicological relevance, which their excessive intake resulted in numerous detrimental health impacts. The concentration of elements present in *Senna* leaves were measured using calibration-free laser-induced breakdown spectroscopy (CF-LIBS) algorithm, and the results were compared to the outcomes of the conventional analytical technique ICP OES. Due to presence of Al, Ca, Cu, Fe, Mg, Mn, P, S, Zn elements in *Senna* leaves, it possess strong antimicrobial and anticancer activity (Mehta et al., 2011). Therefore, the antibacterial and anticancer potentials of the herbal medicine *Senna* leaves extracts were also studied.

2. Methods

2.1. LIBS setup

In this present study, the LIBS technique was applied for the qualitative and quantitative analysis of the Senna leaves samples. LIBS system was employed a fourth harmonic (266 nm), high energy Q-switched Nd-YAG pulsed laser (model: QUV-266–5), which had an output pulse duration of 8 ns, repetition of 20 Hz, and maximum energy up to 50 mJ. The beam was collimated and focused on the sample by a UV convex lens having a focal length of 30 mm, and the plasma was collected by an optical fiber supported by a miniature lens and coupled with a 500 mm spectrograph (Andor SR 500i-A). The sample was kept moving on an X–Y translational stage to avoid forming a deep crust during the LIBS analysis. Detection system (ICCD, model iStar 320 T, 690 × 255 pixels) settings as follows: accumulations number of 25 and a gate width of 2 μs, yielding a better signal/noise ratio, were selected and applied for all the recorded LIBS spectra. An elaborated description of our self-assembled LIBS setup is presented in our group's previous publications and the applied LIBS system in this work is schematically depicted in Fig. S1 (Alhasmi et al., 2015; Gondal et al., 2015).

2.2. Senna leaves assembled for LIBS elemental analysis

Dried leaves of *Senna* were collected from a local market for herbal products in Saudi Arabia. The dried *Senna* leaves were thoroughly cleaned from any adherent dust or contaminant particles, ground into powder. The powder was transferred to a mortar and properly mixed (for approx. 1 h) by a pestle, then sieved with 350 μm mesh screen to obtain a homogeneous powder. This sample characteristic is needed for an efficient laser-sample material interaction translated into better measurements reproducibility and emission intensity enhancement (da Silva Gomes et al., 2011). About 1 g of the leaf powder was placed in a cylindrical pressing die and compressed for 2 min by applying a 10-tons load using a hydraulic press (Specac Ltd., GS15011) to form a circular-shaped pellet (13 mm (width) × 4 mm (height)), as illustrated in Fig. S2. No binder was added to the leaf powder since the pellets were tough to resist the thrust induced by the pulsed laser irradiation. Pellets were kept in a desiccator avoiding contamination and air moisture before conducting the LIBS measurements.

2.3. Senna leaves digestion for the ICP OES inorganic multi elemental detection

Dried *Senna* leaves were quantitatively analyzed using the ICP OES instrument (Agilent's 5110 Vertical Dual View (VDV) ICP OES) for the presence of elements, including Ca, K, Mg, S, P, Na, Al, Si, Fe, Sr, Ba, B, Mn, Ti, Zn, Cu, Cr, Ni, V, Se, Co and As. The leaves powder weighing 300 mg were digested using high pressure and temperature in a specialized microwave (Milestone Inc., Italy). For the acid digestion, a procedure was followed by adding about 5 mL and 1 mL of the nitric acid solution (69%, Sigma Aldrich) and the hydrogen peroxide solution (30% w/v, VWR International), respectively, to the weighted ground *Senna* leaves. The mixture was then subjected to a heating program; first, it was heated to 130 °C for 10 min, and then heated to 240 °C for 10 min, and finally at 240 °C for 15 min. The resultant was cooled down by the chiller to room temperature for 15 min and then diluted to 20 mL using DI water, so being ready to be elementally analyzed using the ICP OES technique. The same procedure was carried out again for the blank samples preparation

2.4. Biological activities

2.4.1. Antibacterial activity

The prepared samples of *Senna leaves* were investigated for its antibacterial activity by applying the agar well diffusion method. The ethanol extract of *Senna leaves* was ranging in the concentration of 50, 100, 150, 200, 250 μg/ml. Test bacterium, *Staphylococcus aureus* ATCC29213 was adopted to study the activity of *Senna* leaves extracts. The bacterium was maintained on nutrient agar media slants at 4 °C and subcultured in nutrient broth for overnight prior to experiment. The bacterial inoculum was prepared by adjusting freshly grown bacteria to 0.5 McFarland standard. Fresh plates of Mueller Hinton agar (MHA) were prepared and evenly spread with 100 μL of adjusted bacterial inoculum to distribute cells evenly. The plates were left for half an hour and later wells of 8 mm size were punched by using sterile cork borer. The punched wells were filled with 100 μL of varying concentration of ethanolic extracts and simultaneously one well in the same plate was filled with 100 μL of sterile Milli-Q water as a negative control. The plates were allowed for diffusion at room temperature for the period of 2 h. Subsequently, plates were transferred to an incubator at 37 °C for overnight. Following the incubation period, the plates were examined to record the inhibition zone (Aldakheel et al., 2020b).

2.4.2. Morphogenesis assessment of Senna extracts

The effect of *Senna* extract on the morphogenesis of *Staphyloccocal* cells was explained by using scanning electron microscope (SEM). The adjusted *Staphyloccocal* cells were treated with 250 μg/ml of extract under the experimental parameters as in previous section. Untreated cells were also included as control (Scio et al., 2012). The treated and untreated cells were subjected to centrifugation at 12,000 rpm for 10 min, the cell pellets were thrice washed with

PBS and initially fixed with 2.5% glutaraldehyde and later fixed with 1% osmium tetroxide. The fixed samples were again washed and dehydrated with ethanol. The samples were placed on the aluminum stubs, dried and coated with gold. The samples were analyzed by SEM at an accelerating voltage of 20 kV.

2.5. Anticancer activity

2.5.1. Treatment of Senna extract on cancerous cell

We have taken two cancer cell lines, human colorectal carcinoma (HCT-116) (ATCC, USA), and human cervical cells (HeLa) (ATCC, USA), to study the impact of *Senna* extract on their viability and proliferation. We have also included the normal cell line of human, such as embryonic kidney cells (HEK-293), (ATCC, USA) to examine the specificity of the *Senna* extract. The cells were cultured and maintained in the DMEM media, L-glutamine (5%), penicillin (1%), streptomycin (1%), FBS (10%), and selenium chloride (1%) as per previously described method (Inoue et al., 2015). The cells were grown in 96 well plates in a 5% CO_2 incubator (Thermo Fisher Scientific, Inc., Waltham, MA, USA) at 37 °C, and 75–80% confluence cells and cell processed for the cell metabolic activity MTT assay (do Nascimento et al., 2020; Inoue et al., 2015).

2.5.2. Cytotoxic assay

The MTT assay was conducted as per the previous studies (Asiri et al., 2019; Khan et al. 2019; Rehman et al., 2019). The cells were treated with *Senna* extract with five different concentrations from 5.0 µg, 15 µg/ml, 20 µg/ml, 30 µg/ml and 40 µg/ml for cancer treatments. The cells were treated for 48 h and processed to examine the cell viability using MTT assay. In the control group, we did not add *Senna* extract. Both the control and *Senna* extract -treated groups treated with 10 µL of MTT (5 mg/ml), and cells were then further incubated in a CO_2 incubator for 4 h. After that, cell culture media was replaced with DMSO (1%), and the 96-well plate was then examined under an ELISA plate reader (Biotek Instruments, USA) at a wavelength of 570 nm. The percentage of cell viability was calculated for the statistical analysis. The data presented as mean (±) standard deviation (SD) obtained from triplicates and one way ANOVA followed by Dennett's post hoc test with GraphPad Prism Software (GraphPad Software, USA) for final statistical analysis

2.5.3. Anti-cancer assay

The cancer cell death was examined by Propidium Iodide (PI) staining assay. Cells were divided into two groups, the control group in which no *Senna* extract were added, whereas, in the experimental group, *Senna* extract (20 µg/ml) was added. Post 48 h treatment, both groups were stained with PI (1.0 µg/mL) for 20 min under a dark environment, and cells were finally washed with PBS and cover slipped. The staining was examined by using Confocal Scanning Microscope (Zeiss, Germany).

3. Results and discussion

3.1. Optimization of the LIBS system

A specific focus and efforts were put on the optimization of two experimental LIBS parameters, the delay time and the pulsed-laser energy which imperatively influence the LIBS analytical performance of the dried *Senna* leaves. Determination of the optimal laser pulse energy is essential as the lower energy results in less ablation rate and lower plasma density, which prevents satisfying the local thermodynamic equilibrium (LTE) condition. With corresponding importance, the time delay of the pulsed laser excitation from the spectrum acquirement should be optimized for the clear demonstration of the emission lines of the atomic or ionic species in the targeted sample. For the initial time spectral reading, the emission is dominated by the featureless broad background (or continuum emission), whereas at longer delay times, the emissions are weak (Aldakheel et al., 2020a). The optimal pulse time delay evaluated for the most elements detected in our dried *Senna* - leaves samples, and was fixed to 320 ns for all the LIBS spectra acquisition. The optimization setting of the LIBS measurements with regard to time delay was performed for the neutral atomic Calcium (Ca) and Magnesium (Mg) spectral lines at wavelength of 422.6 nm and 285.2 nm, respectively. Optical emissions at these two atomic transition lines were acquired for different time delays between 150 and 500 ns. The optimum time delay for Ca I and Mg I spectral lines, giving the temporal maximum intensity yield, is clearly illustrated and presented Fig. S3 and Fig. 1, respectively.

The impact of laser pulse energy on the emission intensity recorded for the spectral lines centered at 422.6 nm and 285.2 nm, which are the fingerprints of the atomic species Ca and Mg, respectively, by varying the pulse energy from 10 to 43 mJ per pulse, are illustrated in Fig. S4 and Fig. 2. The laser irradiance values are also given for these energy values. Detector time delay of 320 ns was set for the experimental energy investigation. The signal intensity was observed to be increasing linearly with energy for the emission lines Ca I (Fig. S4) and Mg I (Fig. 2), a relation validated by the linear fitting with high linear regression/R-squared value ($R^2 = 0.99$) for the two atomic transitions. Increasing the laser excitation energy above 32 mJ for the Ca I and Mg I emission lines leads to nonlinear behavior (saturation), a laser pulse energy of 32 mJ accordingly implied to be the optimal pulse energy for both lines. The optimized value of the laser excitation energy was employed throughout the respective experimental LIBS

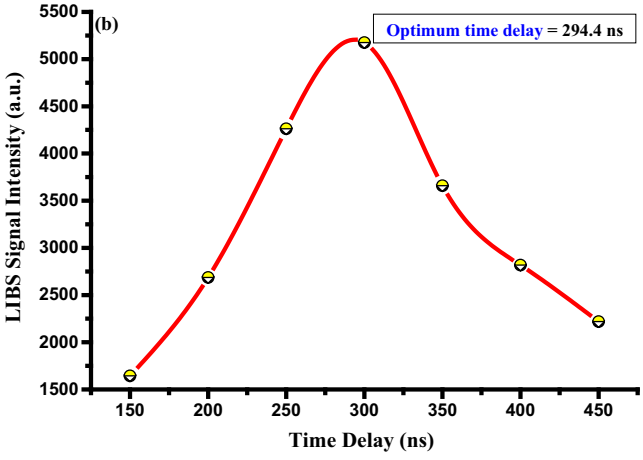

Fig. 1 Representative time delay influence on LIBS emission line intensities using Mg lines 285.2 nm.

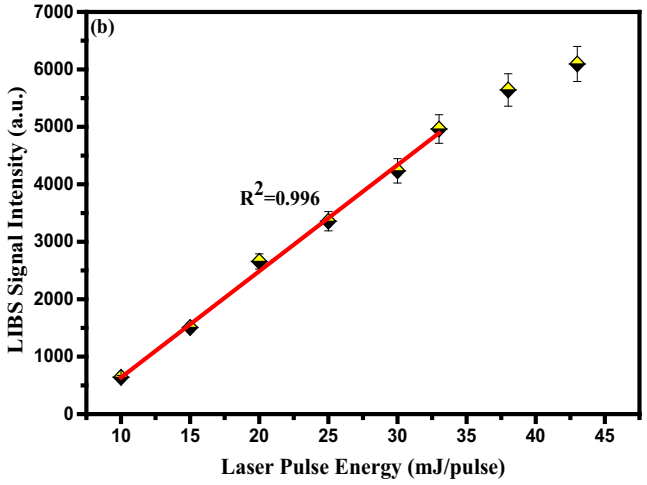

Fig. 2 The representative influence of pulse energy on emission line intensities using of Mg lines peaking at 285.2 nm.

spectral acquisition. The linear dependency represents an increment in the elemental signal intensities due to the enhancement in the mass-ablation rate; however, at a threshold energy value, the emission intensities saturate considering the self-absorption and plasma shielding effects (de Carvalho et al., 2012; Gondal et al., 2012; Mehder et al., 2016).

3.2. Assessment of laser-induced plasma (LIP) parameters

Determination of specific plasma parameters like the electron temperature (T_e) and the electron number density (N_e) is of vital importance for the plasma plume created on the surface of the Senna leaves pellet (El Sherbini and Alamer, 2012). When the collisional processes proceeded with the charged and/or uncharged particles of the laser-induced plasma (LIP) are compensated for the energy dissipation due to the radiative mechanisms, such plasma description is plausible via the thermodynamics distributions. Therefore, the LIP is recognized in the equilibrium state, namely LTE, implying thin plasma and inconsiderable self-absorption effects (Cristoforetti et al., 2010).

LTE condition states that the electron collisions should be the dominating process for the population and de-population of the atomic energy levels, and this demands sufficiently high electron number density (Hussain and Gondal, 2008). The postulated criterion of McWhirter (Cristoforetti et al., 2013; Hussain and Gondal, 2008; Gondal et al., 2012) was employed to provide the lower boundary of the plasma electron number density (N_e) for *Senna* leaves. For a hypothesized LTE, the electron temperature (T_e) is another important parameter that characterizes the plasma of *Senna* leaves, and the most accepted approach enables its determination is the Boltzmann plot method (Hussain and Gondal, 2008; Gondal et al., 2012). This method uses different spectral transitions of the same species corresponding to an individual element and were chosen with definite criteria (Aldakheel et al., 2020a; Tognoni et al., 2007).

There are many transition lines of Ca covering a wide wavelength range of 200–900 nm, yielding a proper T_e determination. Therefore, T_e was estimated for the laser prodcued plasma on the laser-ablated surface of *Senna* leaves pellets by using well-isolated and resolved neutral Ca atomic lines at 428.9, 430.7, 442.5, 527.0, 585.7, 616.2, and 649.3 nm. The corresponding spectroscopic details of these transition lines from the atomic spectroscopy database (NIST) are conferred by Table S1. Fig. 3 displays the linear Boltzmann plot using these Ca transition lines identified in the recorded spectra. The T_e value of 11841.4 ± 473.7 K derived from the slop of the straight-line. An R^2 value of 0.99 indicates the best fitting of the spectroscopic data, and in consequence, the LTE state was validated for the plasma, which obeys the Boltzmann distribution. The electron temperature was recalculated for the confirmation purposes incorporating the spectrally observed ionic iron (Fe) lines centered at 256.2, 259.8, 260.7, 273.9, 274.6, 274.9, and 275.5 nm, and a T_e value of 12055 K was obtained, as shown in Fig. 3. Stark effect is the predominant line-broadening scheme as against Doppler and other impact pressure broadening schemes for plasma generated by laser irradiation that is of high electron density in the range 10^{14}–10^{18} cm^{-3} (Harilal et al., 1997; Hegazy et al., 2014). Stark effect, owing to the emitters collisions, i.e., ions and atoms, with electrons and ions, is the main contributor to the line width broadening, and its influencing degree is in direct correlation to the electron density (Aragon et al., 2001). Thereupon, the plasma electron number density (N_e) can be predicted using the Stark-broadening method (Hussain and Gondal, 2008; Gondal et al., 2012; Sarkar and Sing, 2017), and based on the full width at half maximum (FWHM) for an isolated and non-hydrogenic neutral or singly-ionized transitions, neglecting a contribution from the ionic-impact broadening.

The electron number density (N_e) was evaluated from the Lorentzian-fitted Ca I line peaked at 442.5 nm, corresponding to the $3p^6\ 4s4p\ ^3P_0^o \rightarrow 3p^6\ 4s4d\ ^3D_1$ transition. The spectral lines utilized for the measurement of the N_e by the Stark broadening method are inquired to be freed from the self-absorption effect (El Sherbini and Alamer, 2012; Hegazy et al., 2014). The non-resonant Ca I line fixed at 442.5 nm was perfectly fitted exploiting the Lorentzian function, denoting no affection of self-absorption (Li et al., 2014). The full-width at half maximum (FWHM) was measured for that line, as shown in

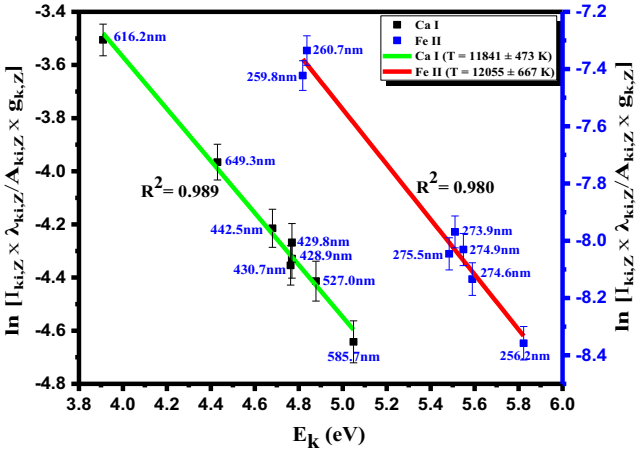

Fig. 3 Boltzmann plot used eight neutral Ca and seven ionic Fe spectral lines detected in LIP created on the surface of our targeted (dried *Senna* leaves) samples for T_e determination.

Fig. 4. Doppler width was measured from the T_e of 11 841.4 K for the neutral Ca atomic transition at 442.54 nm as 0.005 nm. Thus, the contribution of Doppler broadening was neglected as its width is very small (Shaikh et al., 2007). Considering the FWHM-value and the estimated Stark-broadening parameter 0.063 Å for the Ca I line (442.5 nm) (Aldakheel et al., 2020a), the calculated N_e value then was 6.08×10^{16} cm^{-3}. The experimental value of N_e measurement was higher than the lowest calculated N_e limit (3.8×10^{15} cm^{-3}). This result ensures the plasma thinness and it's following to the stipulated conditions of LTE, which thereby decreases the possibility of spectral line distortion associated with the self-absorption effect.

3.3. Elemental analysis of Senna leaves using the LIBS technique

As long as the optimization of the quality status of LIBS measurement resolved for the *Senna* leaves samples, and the optical thinness characterized the plasma generated on the surface of the pellets, spectra with minimized continuum background ensured that enhanced the detection rate. All LIBS spectra constructed using an average of 25 accumulations from at least three surface points. That carried out to reduce the possible influences from sample heterogeneity and fluctuations among laser pulses (Liu et al., 2015), which further improved the LIBS signal-to-noise ratio. LIBS spectra acquired from multiple regions of the wavelength scale, 245–365 nm, 390–450 nm, and 540–780 nm, as the main wavelength ranges were illustrated in Fig. 5a-c, 6a-c, and 7a-c, respectively. The acquired spectra demonstrated an impressive array of spectral lines from atomic (I) and singly-charged ionic (II) species that lead to the qualitative identification of the elements present in the characterized plasma of our tested *Senna* samples. Lines identification through the NIST atomic spectral database notified diversity in elements composing *Senna leaves* such as Ca, K, Mg, S, P, Na, Al, Si, Fe, Sr, B, Ba, Mn, Ti, Zn, Cr, Co, Ni and V. Each element preset by a pattern of characteristic emission lines. At least two or three different persistent spectral lines monitored to verify the element presence. Emission lines of the organic elements like C and O were detected for the *Senna* samples, ensuring their organic structure and the capability of the LIBS system to detect lighter elements over other standard analytical techniques (Tripathi et al., 2015).

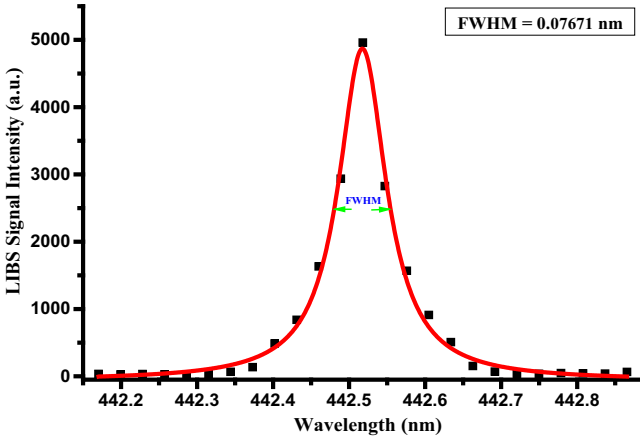

Fig. 4 Lorentzian-fitted stark-broadened line profile of the Ca I spectral line at 442.5 nm respective to the transition configuration of ($3p^6$ $4s4p$ $^3P^o_0 \rightarrow$ $3p^6$ $4s4d$ $^3D_1$).

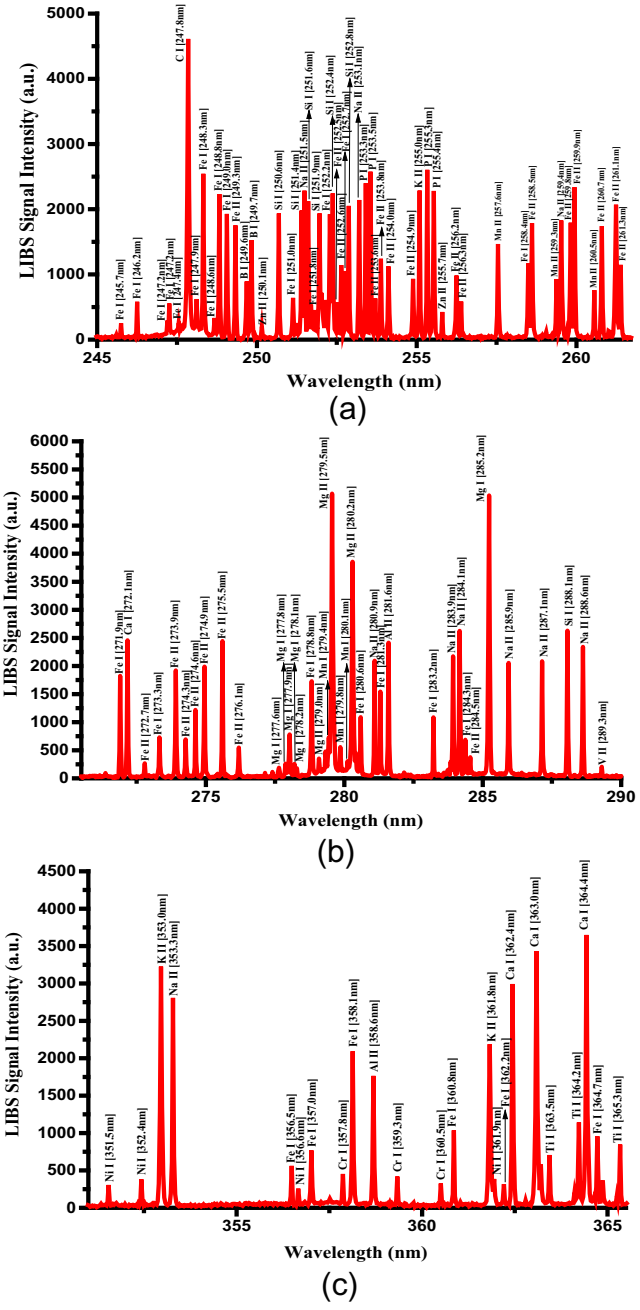

Fig. 5 Optical emission spectra of the dried *Senna* leaves in the wavelength range 245–365 nm.

Table S2 represents some of the transitions identified for the elemental analytes composing of the dried *Senna* leaves and their related emission intensities. LIBS intensities unveiled the nutritious-enriched *Senna* leaves from Ca, K, Mg, S, P, Na, Si, and Fe. Al, Sr, B, Ba, Mn, Zn, and Cr elements were found in a significant amount, and this may pose a serious health risk to humans when consumed orally. It is of medicinal importance that potentially toxic elements like cadmium (Cd), lead (Pb), and arsenic (As) were not detected in dried *Senna* leaves. The availability of Ca and Mg in *Senna* leaves makes it an appropriate

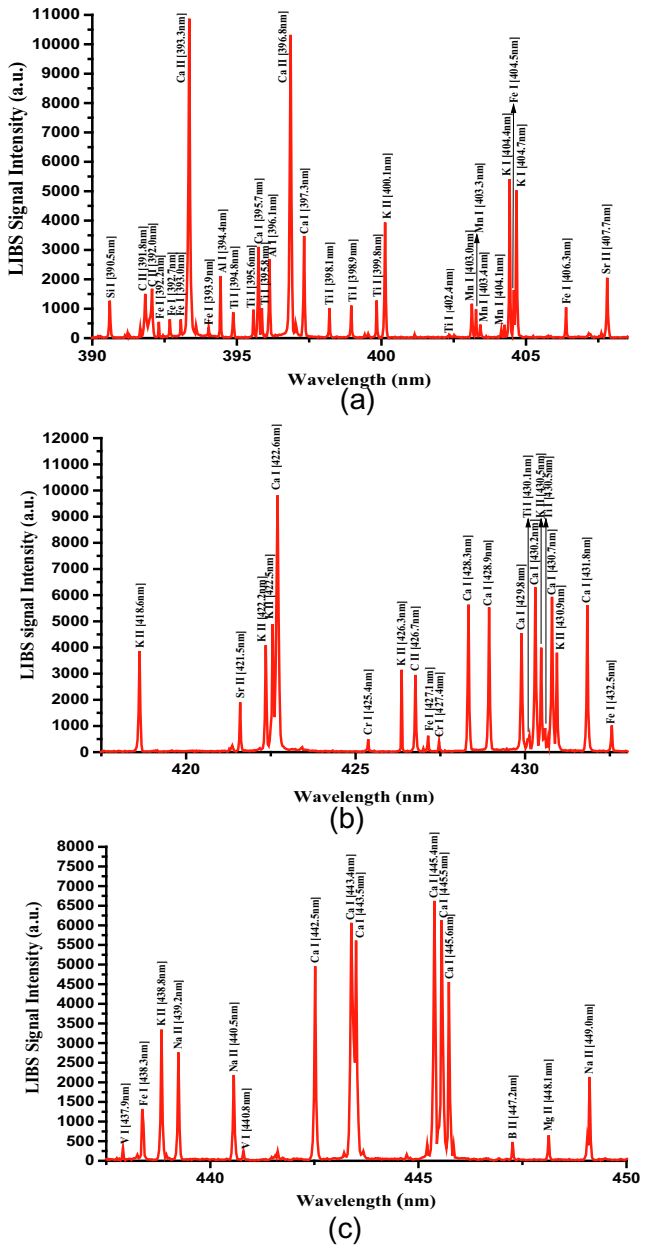

Fig. 6 a-c. Optical emission spectra of the dried *Senna* leaves in the wavelength range 390–450 nm.

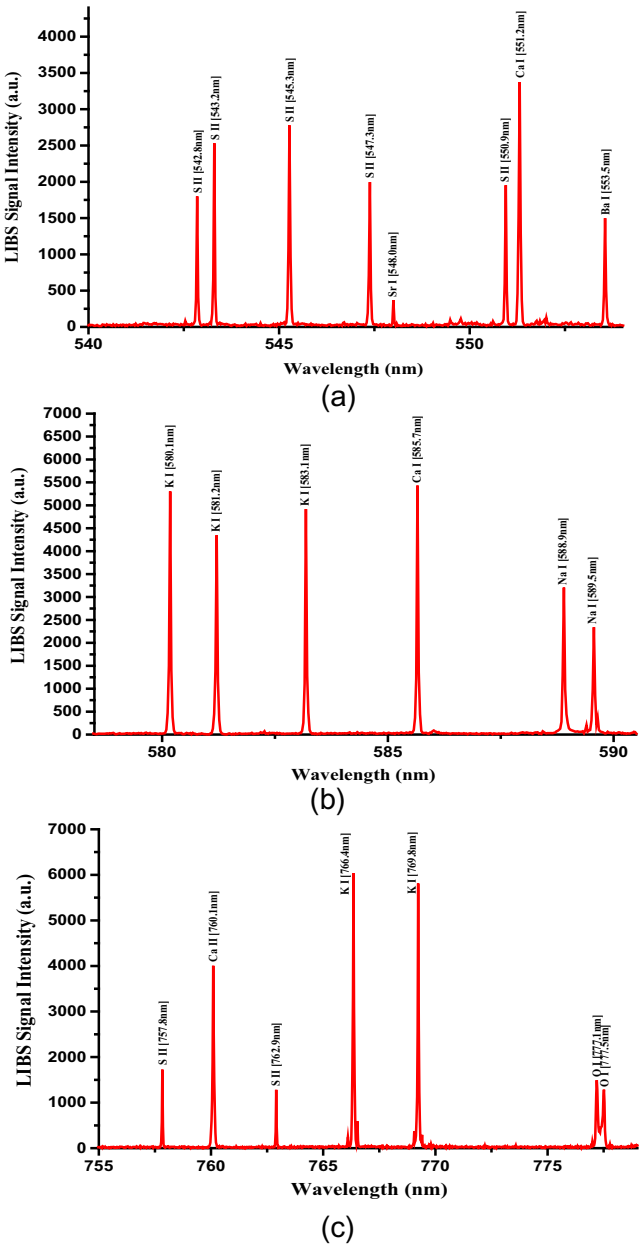

Fig. 7 a-c. Optical emission spectra of the dried *Senna* leaves in the wavelength range 540–780 nm.

treatment for diabetic patients and those with liver damage; thereupon, it could support the therapeutic use of *Senna* leaves in those patients. The aqueous extract of *Tinnevelly Senna* leaves showed antidiabetic/hypoglycemic and hypolipidemic effects in rats developed type-2 diabetes mellitus (T2DM) (Jani and Goswami, 2020; Osman et al., 2017). Moreover, *Tinnevelly senna* leaves increased the levels of free-radical scavengers like GSH, GPX, CAT, and SOD in diabetic rats (Osman et al., 2017). High-fat diet (HFD) containing 1.0% calcium markedly reduced glucose surges and HOMA-IR score in the HFD-induced obese rats (Das and Choudhuri, 2020). Pre-diabetic (Guerrero-Romero et al., 2015) or diabetic (Rodríguez-Morán and Guerrero-Romero, 2003) subjects with hypomagnesemia have an ameliorated glycemic profile and insulin sensitivity status after receiving magnesium supplementation.

Tinnevelly senna leaves revealed a hepatoprotective property, i.e., a reduction in hepatic function biomarkers and an increment in the antioxidants activities, against the liver injury induced in rats by carbon tetrachloride (CCl_4) (Bellassoued et al., 2019). Calcium supplementation demonstrated similar impacts and urged a hepatoprotective action concerning non-alcoholic fatty liver diseases (NAFLD) development (Das and Choudhuri, 2019). Magnesium also plays a vital role in the protection of the hepatic cells function as its deficiency has been linked with lipid peroxidation (Eidi et al., 2013). There was a noticeable reduction in the serum potassium level after receiving sennosides cathartic for the colonic cleanse examination (Ritsema and Eilers, 1994). Therefore, potassium-enriched *Senna* leaves might maintain the potas-

sium homeostasis for not more than the recommended 1 to 2 weeks (Blumenthal et al., 2000).

The possibly essential Boron in the human body found boosting bone growth, brain activities (Khaliq et al., 2018; Nielsen, 2014), and also exhibits antioxidant effects (Khaliq et al., 2018). B intoxication in humans arose after oral exposure to more than 84 mg/kg of boron (Uluisik et al., 2018); however, B levels in *Senna* leaves (43 mg/kg) were markedly higher **than** about 0.4 mg/kg-b.w./d set as the tolerable upper B-intake level for adults (Nielsen, 2014). Mn is essential for brain glutamine synthesis, energy metabolism, redox catalysis via manganese superoxide dismutase (Mn-SOD), etc. However, excessive brain exposure to Mn may be neurotoxicant (Sigel et al., 2013). *Senna* leaves contain 34 mg/kg of Mn that exceeds the safe recommended dietary intake for adults of 0.03–0.07 mg/kg-b.w/day (Nordberg, 2014). Interestingly, there was a high level of the non-essential Sr in *Senna* leaves (182 mg/kg) contrasting the minimal risk level (MRL) set for the oral stable-Sr dosage of 2 mg/kg.b.w.day (Coelho et al., 2017), which gives rise to modulations in the bone mineralization profile (Pilmane et al., 2017). Al and Ba elements with no clear evidence of their role in the human body present in higher concentrations in *Senna* leaves than the recommended oral intake of 0.3 (Willhite et al., 2014) and 0.2 (Kravchenko et al., 2014) mg/kg-b.w./d for adults, respectively. *Senna* leaves contain Zn of a quantity (9.3 mg/kg) plausibly surpassed the daily upper intake limit of 40 mg in adult subjects, and the excessive zinc dietary intake leads to an impaired immunological response and copper deficiency (Trumbo et al., 2001). Although there is insufficient scientific data on the adverse health influences from the high food or supplementation intake of soluble-Cr (III) salts to establish an upper intake level (UL), caution should be taken with Cr (III) intake. Cr was detected in Senna leaves with 3.5 mg/kg and may pose a health threat with an amount exceeding the extrapolated adequate intake for adult women and men of 25 and 35 μg/day, respectively (Trumbo et al., 2001). Indeed, there were isolated incidents of the detrimental effects due to chromium (III) picolinate supplementation (≥600 μg/day) (Vincent, 2003). To conclude with, elemental analytes, such as Al, Sr, B, Ba, Mn, Zn, and Cr, were conjectured to be toxic in *Senna* leaves. Thereupon, the treatment protocol based on *Senna* leaves should be initiated on taking an effective lowest dose of that traditional medical remedy for the shortest period of time.

3.4. Quantitative evaluation of the elements present in Senna leaves using LIBS and ICP OES techniques

Senna leaves were digested using an acid-oxidant mixture with a requisite high-degree of purity and then quantitatively analyzed by ICP OES for 24 elements: Ca, K, Mg, S, P, Na, Al, Si, Fe, Sr, B, Ba, Mn, Ti, Zn, Cr, Cu, Ni, V, As, Se, Cd, Co, and Pb. The measured concentrations of the elements in the *Senna* leaves using ICP OES method are cited in Table S2. Intriguingly, the non-detection of As, Se, Cd, Co, and Pb elements in the tested *Senna* leaves samples by the standard analytical ICP OES method confirmed the LIBS findings. There is a correspondence between our study and the work (Levine et al., 2004) in the appearance of Al, Ba, Ca, Cu, Fe, Mg, Mn, Na, Sr, Zn, and V elements and the nonappearance of the toxic Cd and Pb elements. However, Cr was found only in our samples. Validation of the predicted elemental presence throughout the qualitative analysis of the LIBS technique was fulfilled with the ICP OES outcomes, as clearly shown in Table S2. The total elements specified by the LIBS analysis to constitute the *Senna* leaves samples, such as Ca, K, Mg, S, P, Na, Al, Si, Fe, Sr, B, Ba, Mn, Ti, Zn, Cr, Cu, Ni, and V measured at different concentrations by the ICP OES as following 26193, 9829, 3499.5, 2311, 1516.9, 968, 574.8, 550.6, 477.7, 182.6, 43.5, 35, 34, 21.9, 9, 3.5, 3, 1.9, and 1.5 mg/kg, respectively. The ICP OES results manifested higher levels of Ca, K, and Mg, sequentially, in *Senna* leaves, which relatively are analogous to their emission intensities conferred with the LIBS spectra. The concentration of all these detected elements was determined as discussed by using the CF-LIBS method, and its quantification potential discerned by the comparison with the ICP OES results.

3.5. CF-LIBS approach for quantification analysis

For quantifying the elements in *Senna* leaves sample, the algorithmic CF-LIBS technique was used. This method avoids the matrix effect impediments (Tognoni et al., 2007). There are two main conditions to apply CF-LIBS, i.e., plasma necessarily characterized as optically thin with insignificant self-absorption and plasma in LTE while acquiring the LIBS spectra. In Section 3.2 plasma temperature T_e calculated and electron number density N_e was high enough to ensure the LTE. The integrated intensity of the detected emission line is given by:

$$I_{\lambda}^{ki} = FC_sA_{ki}\frac{g_k}{U_s(T)}\mathbf{exp}\left(\frac{-E_k}{K_BT}\right) \quad (1)$$

where k and i are the indices of the upper and lower transition levels, λ is the wavelength corresponding to the transition between the upper energy level E_k and lower energy level E_i, F is an experimental parameter that takes into account the optical efficiency of the collection system, as well as the total plasma density, and C_s is the concentration of the emitting species s. A_{ki} is the transition probability for spontaneous emission from state k to i, g_k is the degeneracy of the k level, K_B is the Boltzmann constant, T is the plasma temperature, and Us (T) is the partition function of the emitting species at the plasma temperature T, which can be determined by the equation:

$$U(T) = \sum g_k \exp\left(\frac{-E_k}{K_BT}\right) \quad (2)$$

The NIST standard reference database was used to obtain the atomic parameters of the spectral lines. F, Cs, and T values possibly calculated using the experimental findings available from Tables S1 and S2. After that, the F parameter can be derived by the normalization of the total concentrations of the constituent species.

$$\sum_s \mathbf{C_s} = \frac{1}{\mathbf{F}}\mathbf{U_s(T)}\exp(\mathbf{q_s}) = 1 \quad (3)$$

where $q_s = \ln\left(\frac{C_sF}{U(T)}\right)$. Lastly, the species concentration of the *Senna* leaves can be then given by:

$$C_s = \frac{1}{F}U_s(T)\exp(q_s) \quad (4)$$

Summation of the neutral and singly-ionized species, as depicted by Eq. (5), gives the concentration of an element in *Senna* leaves.

$$C_{i(tot)} = C_s(I) + C_s(II) \quad (5)$$

Table 1 presents the comparison between CF- LIBS and ICP OES results for Senna leaves. The CF-LIBS results are in high concurrent with the standard method of ICP OES.

3.6. The comparative figure of CF-LIBS and ICP OES results

Before commencing LIBS measurements, stabilizing the laser device by warming it up for a sufficient time to avoid laser pulse fluctuations is recommended. The relative standard deviation of the LIBS measurements decreases as the laser shots number increases; thence, an average of 25 accumulations was used to construct the LIBS spectrum. The relative accuracy (RA) is given by

$$RA = \frac{|d| + SD \times \frac{t_{0.975}}{\sqrt{n}}}{M} \quad (6)$$

where d is the LIBS measurement difference from that of ICP OES technique, SD is the standard deviation of LIBS measurements, M is the ICP OES measurement, n is the LIBS measurements number, and $t_{0.972}$ is the t-value at a 2.5% error confidence. RA delivered for our CF-LIBS setup, as depicted in Table 1, takes values of 0.07–0.49, denoting a quiet acceptance level for any efficient instrumental system.

The relative standard deviation is given by:

$$RSD = \frac{SD}{X} \times 100 \quad (7)$$

where X is the mean of n measurements. RSD values were pretty small, as shown in Table 1, which indicates the precise of CF-LIBS calculations.

3.7. Biological activities study

3.7.1. Antistaphyloccal activity and morphogenisis study

The antibacterial efficacy of the *Senna* leaves extract was investigated on Gram-positive bacterium *Staphyloccocus aureus* by agar well diffusion method, wherein the suppressed areas due to biological activity surrounding the wells with extracts, were measured. This hollow zone was formed by the active diffusion of the phytochemical elements occurring in the *Senna* leaves extract. The obtained results depicted the antibacterial action of *Senna* leaves extract on *S. aureus*. In Fig. 8, the *Senna* leaves extract exhibited concentration-dependent inhibition of the test bacterium, presenting the inhibition zones ranging from 10 to 18 mm. The varying diameters of inhibition zone were observed with the extract contents of 250 and 50 μg/mL, however no inhibition was observed with 25 μg/mL (Fig. 8b).

The structural changes in *Staphylococcal* cells treated with *Senna* extracts were estimated using SEM. The untreated cells were seen as normal cocci shaped with regular appearing cell surfaces (Fig. 9 a). The *S. aureus* treated with *Senna* leaves extract were observed as damaged with reduction in cell number and having significant changes of the cell surfaces (Fig. 9 b). *Staphylococcus aureus* is a wound infecting organism that may lead to endocarditic/ toxic shock syndrome and septicemia. The ethanolic leaf extracts of *Senna* showed antibacterial activity by the technique agar well diffusion method. This activity could be owed to various phytochemicals like, flavonoids, phenols, tannins, alkaloids, saponins, and other aromatic constituents of plants including *Senna* (Campos et al., 2016; Viswanathan and Nallamuthu, 2012). These constituents basically act for their own defense phenomenon against phytopathogens, insects and other predators. The current study indicated the existence of many active elemental constituents which could be the possible reason for the obtained antibacterial activity. These phytoconstituents are known to act by various mechanisms in order to attain the antimicrobial property.

Table 1 Comparative results of CF LIBS and ICP OES methods of elements present in *Senna* leaves.

Elements detected in *Senna* samples	Comparison of LIBS and ICP OES, and RA			RSD (%)
	CF-LIBS mg/kg	ICP OES mg/kg	RA	
Ca	26158.15	26193.35	0.10	1.75
K	9835.19	9829.17	0.09	1.05
Mg	3479.67	3499.54	0.15	1.43
S	2301.45	2311.49	0.07	1.08
P	1530.14	1516.95	0.22	1.97
Na	986.33	968.37	0.31	2.11
Al	562.54	574.85	0.37	2.24
Si	539.67	550.66	0.47	2.23
Fe	458.86	477.72	0.48	2.97
Sr	181.16	182.63	0.07	1.04
B	45.92	43.56	0.39	2.34
Ba	32.37	35.16	0.31	2.44
Mn	37.34	34.20	0.50	2.84
Ti	24.74	21.95	0.42	3.14
Zn	9.39	9.36	0.11	1.36
Cr	4.42	3.54	0.46	1.68
Cu	4.12	3.23	0.49	3.13
Ni	1.71	1.94	0.29	2.17
V	1.16	1.5	0.26	2.65

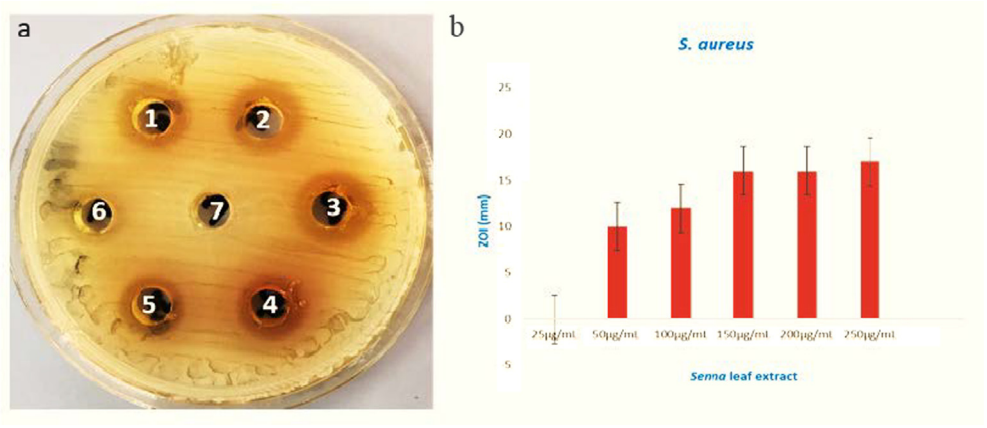

Fig. 8 (a) The MHA plate and (b) graphical presentation of the zones of inhibition in millimeters (mm) examined against *S. aureus* after treatment of different concentrations of *Senna* leaves extract. (1, 2, 3, 4, 5, 6 representing 25, 50, 100, 150, 250 µg/mL extract, respectively, and 7 representing sterile water as control.

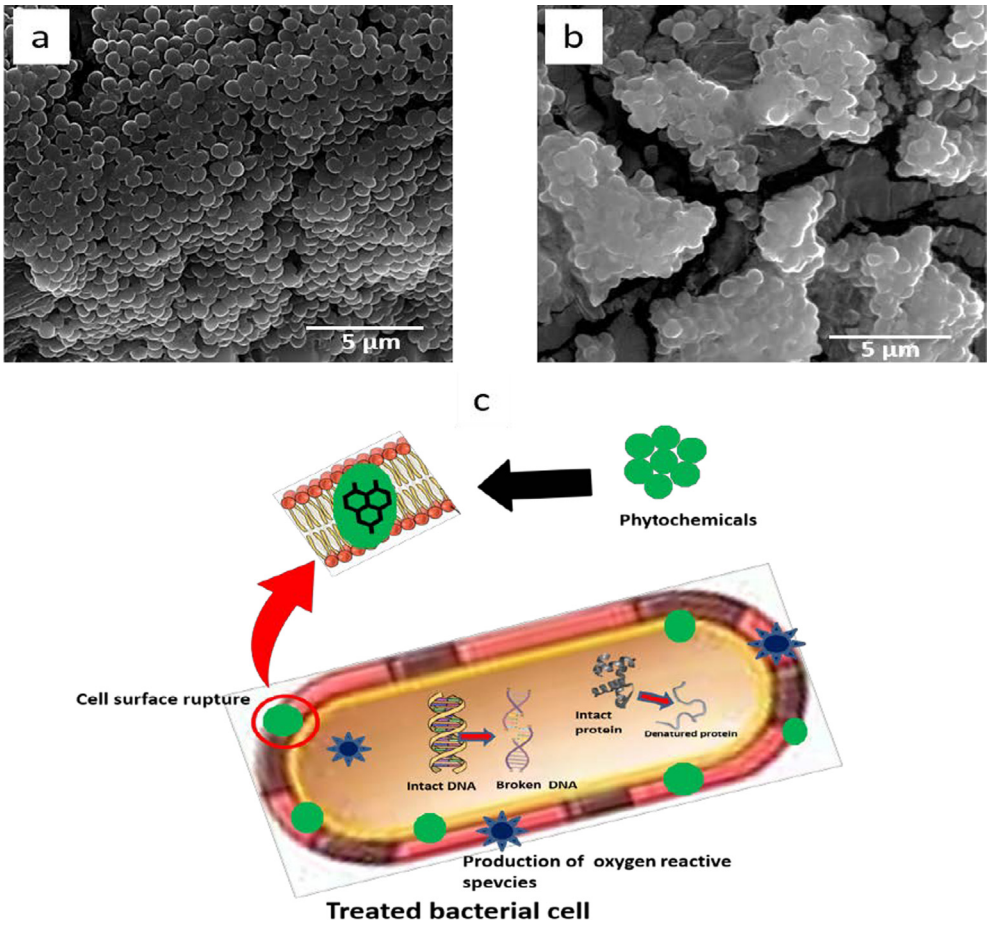

Fig. 9 The representative SEM micrographs of *S. aureus* (a) untreated *S. aureus* as control (b) treated with 250 µg/mL of *Senna* leaves extract, (c) The probable antibacterial mechanism of the phytomolecules of *Senna* leaves extract.

They bind to proteins and intervene in the process of translation (Aldakheel et al., 2020b). The ability to complex with the extracellular and soluble proteins associated with bacterial cell surfaces leads to disruption of cellular surfaces that ultimately cause leakage of cell contents like proteins and several enzymes from the cell (Fig. 9c). This study goes in agreement with number of previous studies that have demonstrated the antimicrobial action of various species of *Senna* plant extracts (do Nascimento et al., 2020; Inoue et al., 2015; Scio et al., 2012).

3.7.2. Anticancer activities

The impact of *Senna* leaves extract on colon cancer cells (HCT-116) and cervical cancer (HeLa) cells was examined. The cell viability assay confirmed a significant decrease in the cell viability after the treatments of *Senna* leaves extract (Fig. 10). We have also calculated the inhibitory concentration (IC_{50}) value for the various extracts concentrations (25 µg/ml, 50 µg/ml, 100 µg/ml, 150 µg/ml, 200 µg/ml, and 225 µg/ml). We have found that IC_{50} value for HCT-116 cells were 13.5 µg/ml, 17.5 µg/ml, 21.5 µg/ml, 22.5 µg/ml, 26 µg/ml and 33.5 µg/ml and for HeLa cells 15.25 µg/ml, 21.25 µg/ml, 23.5 µg/ml, 262.5 µg/ml, 36.25 µg/ml, and 39.50 µg/ml. We have also tested the impact of *Senna* leaves extract on non-cancerous cells; HEK-293, we did not find any significant inhibitory action on HEK-293 cells. This is the first study demonstrating impact of *Senna* leaves extract against HCT-116 cells. The concentration of different elements present in *Senna* leaves such as Al, Ca, Cu, Fe, Mg, Mn, P, S, and Zn, was shown to possess anticancer activity (Mehta et al., 2011). *Senna velutina* leaf extract found to contain antioxidant and anti-leukemic potentials. When extracts of *Senna* leaves were treated with Leukemia human cell lines Jurkat and K562, the IC_{50} values for Jurkat cells were 27.6 µg/ml, which was found to be better inhibitor then erythroleukemic cell line K562 (67.5 µg/ml) (Campos et al., 2016).

The treatment of *Senna* leaves extract caused significant decreased in the number of HeLa cells, as shown by MTT assay, whereas when stained with Propidium iodide (PI) staining, we have found that number of dead cells stained with PI is higher in the *Senna* leaves extract -treated cells (Fig. 11 b) as compared to control cells (Fig. 11 a). Propidium Iodide is membrane impermeant dye, which prevents DNA binding in

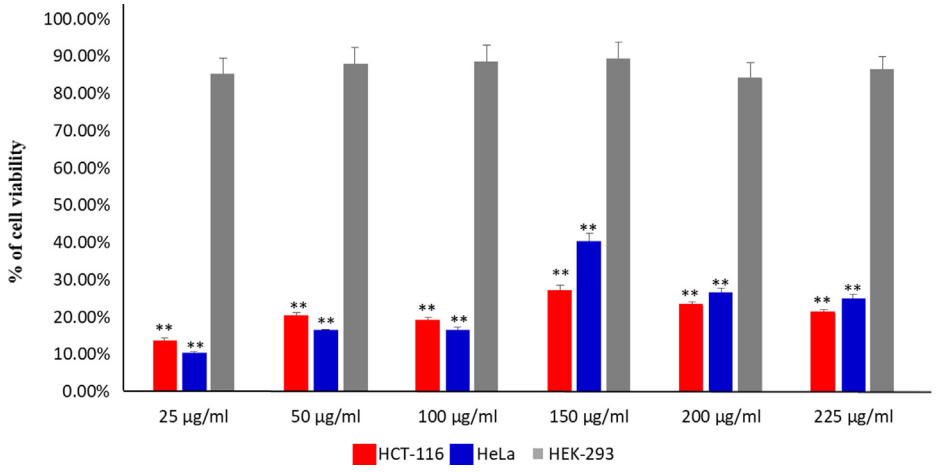

Fig. 10 Cancer cell viability by MTT Assay: It shows the impact of treatment of *Senna* leaf extract on colon cancer cells (HCT-116) viability post 48 h treatment. Data are the means ± SD of three different experiments. Difference between two treatment groups were analyzed by student's *t* test where **p < 0.01), p-values were calculated by Student's *t*-test.

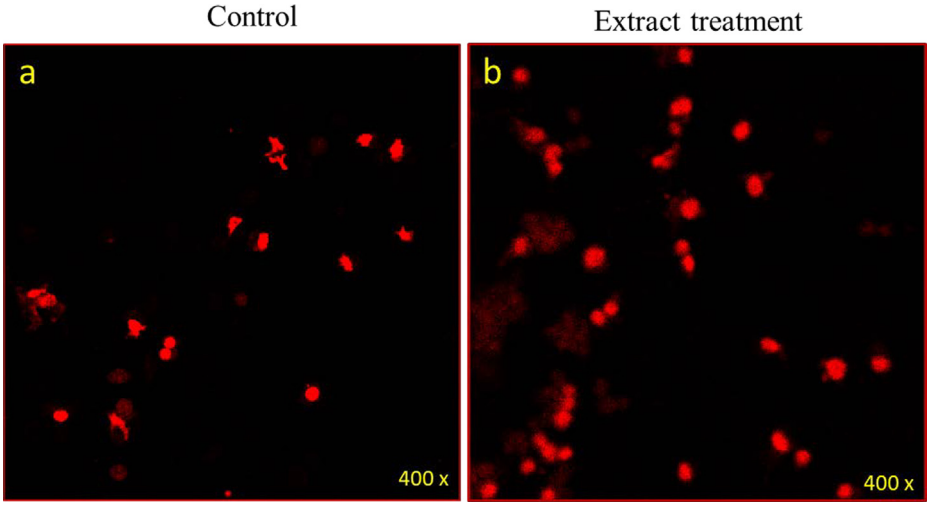

Fig. 11 Cancer cell death due treatment of *Senna* leaf extract: It shows the impact of treatment of *Senna* leaf extract on colon cancer cells (HCT-116) stained with Propidium iodide (PI) post 48 h treatment. In this figure, (a) represents the control cell with few cell death and (b) a significant number of cancer cells due to (20 µg/ml) treatment.

viable cells, allowing identification of dead cells in a population cells. The cancer cell death is due to programmed cell death or apoptosis. Previously we have shown that treatment of nanoparticles caused the significant loss of cancer cells due to programmed cell death (Asiri et al., 2019; Khan et al., 2018a, 2018b).

4. Conclusion

Tinnevelly senna leaves traditionally popularized as a strong purgative and herbal drug due to its constituents of bioactive compounds, which emphasizes on the variability of its medicinal purposes. However, we emphasized here that discovering the elemental composition of the *Senna* leaves may result in optimal medicinal value and therapeutic potentials since numerous elements are of vital biochemical significance and contribute efficiently to the well-being of humans and their health. Thus, a rapid, safe, and accurate atomic analytical technique like LIBS is imperative to provide the element content of medicinal herbs. LIBS spectra showed spectral lines of different elements Ca, K, Mg, S, P, Na, Al, Si, Fe, Sr, B, Ba, Mn, Ti, Zn, Cr, Cu, Ni, and V. The quantitative elemental analysis via CF-LIBS of the dried *Senna* leaves demonstrated its content of different nutrient elements such as Ca, K, Mg, S, P, Na, Si, Fe, Cu, Ni, and V with the estimated concentrations of 26158.15, 9835.19, 3479.67, 2301.45, 1530.14, 986.33, 539.67, 458.86, 4.12, 1.71, and 1.16 mg/kg. *Senna* leaves contained a Ti element that existed at an amount of 24.74 mg/kg. Additionally, LIBS spectra uncovered some elements that might pose a threat to human health in *Senna* leaves like Al, Sr, B, Ba, Mn, Zn, and Cr with the amounts 562.54, 181.16, 45.92, 32.37, 37.34, 9.36, and 4.42 mg/kg. Before commencing the LIBS measurements, several parameters were optimized to confirm the optical thinness characteristic for the plasma generated on the *Senna* leaves samples, which warrants a reliable quantitative analysis using a self-developed CF-LIBS method. The elemental contents in *Senna* leaves estimated by CF-LIBS was in good concordance with that measured by a standard ICP-OES method. The bactericidal efficacy of the *Senna* leaves extract against S. aureus by AWD assay and morphogenesis by SEM, revealed significant activity and the morphogenesis inflicted to the test bacterium. The anticancer activity was examined where different concentration of *Senna* leaves extracts were tested on human colorectal carcinoma cells (HCT-116) and human cervical (HeLa) using MTT assay and Propidium iodide (PI) staining. We have calculated the inhibitory concentration (IC50) value for the various extracts concentrations (25 µg/ml, 50 µg/ml, 100 µg/ml, 150 µg/ml, 200 µg/ml, and 225 µg/ml). We have found that IC_{50} value for HCT-116 cells were 13.5 µg/ml, 17.5 µg/ml, 21.5 µg/ml, 22.5 µg/ml, 26 µg/ml and 33.5 µg/ml and for HeLa cells 15.25 µg/ml, 21.25 µg/ml, 23.5 µg/ml, 262.5 µg/ml, 36.25 µg/ml, and 39.50 µg/ml. Both MTT and PI analysis showed that *Senna* leaves extract induced profound inhibition on the both HCT-116 growth and proliferations. Additionally, *Senna* leaves extract did not exert an inhibitory influence on normal (HEK-293), which is non-cancerous cells. We suggest that the extract specifically targets the cancerous cells, which could be highly beneficial for the development of future safe anticancer and antibacterial drugs. Future *in vivo* studies may be designed to further examine and validate the potentials of *Senna* leaves extracts in the treatments of bacterial infections and cancer cells.

Author Contributions

MAG, MAA, FAK conceptualized, designed the study; MAG, MAA supervised the study, RKA MMN, SR, and ZA participated in data acquisition and data analysis; MAG, MAA, RKA, and FAK and were involved in writing, reviewing and editing the manuscript. All authors reviewed the final draft and agreed to the publication of this manuscript.

Declaration of Competing Interest

The authors declare that they have no known competing financial interests or personal relationships that could have appeared to influence the work reported in this paper.

Acknowledgements

The authors are thankful to the Deanship of Research, King Fahd University of Petroleum and Minerals for supporting this work. We acknowledge the financial support received from Deanship of Scientific Research, Imam Abdulrahman Bin Faisal University, Dammam, Saudi Arabia to conduct the experiments. Prof. Gondal is thankful to K.A.CARE for fellowship.

Appendix A. Supplementary material

Supplementary data to this article can be found online at https://doi.org/10.1016/j.arabjc.2021.103451.

References

Ahmed, M.M., Ahmed, M.M., Said, Z.S., Montaser, S.A., El Tawil, G.A., 2018. Antioxidant and antimutagenic properties of calcium sennosides in γ-Irradiated human blood cultures. Int. J. Radiat. Res. 16 (3), 323–332.

Ahmed, S.I., Hayat, M.Q., Tahir, M., Mansoor, Q., Ismail, M., Keck, K., Bates, R.B., 2016. Pharmacologically active flavonoids from the anticancer, antioxidant and antimicrobial extracts of Cassia angustifolia Vahl. BMC Complement. Altern. Med. 16 (1), 460.

Alhasmi, A.M., Gondal, M.A., Nasr, M.M., Shafik, S., Habibullah, Y. B., 2015. Detection of toxic elements using laser-induced breakdown spectroscopy in smokers' and nonsmokers' teeth and investigation of periodontal parameters. Appl. Opt. 54 (24), 7342–7349.

Aldakheel, R.K., Gondal, M.A., Nasr, M.M., Almessiere, M.A., Idris, N., 2020a. Spectral analysis of Miracle Moringa tree leaves using X-ray photoelectron, laser induced breakdown and inductively coupled plasma-optical emission spectroscopic techniques. Talanta 121062.

Aldakheel, R.K., Gondal, M.A., Nasr, M.M., Dastageer, M.A., Almessiere, M.A., 2020b. Quantitative elemental analysis of nutritional, hazardous and pharmacologically active elements in medicinal rhatany root using laser induced breakdown spectroscopy. Arab. J. Chem. 102919.

Andrade, D.F., Guedes, W.N., Pereira, F.M.V., 2018. Detection of chemical elements related to impurities leached from raw sugarcane: use of laser-induced breakdown spectroscopy (LIBS) and chemometrics. Microchem. J. 137, 443–448.

Andrade, D.F., Pereira-Filho, E.R., Konieczynski, P., 2017. Comparison of ICP OES and LIBS analysis of medicinal herbs rich in flavonoids from Eastern Europe. J. Braz. Chem. Soc. 28, 838–847.

Aragon, C., Bengoechea, J., Aguilera, A.J., 2001. Influence of the optical depth on spectral line emission from laser-induced plasmas. Spectrochim. Acta B 56 (6), 619–628.

Asiri, S.M., Khan, F.A., Bozkurt, A., 2019. Delivery of conjugated silicon dioxide nanoparticles show strong anti-proliferative activities. Appl. Biochem. Biotechnol. 189 (3), 760–773.

Bellassoued, K., Hamed, H., Ghrab, F., Kallel, R., Van Pelt, J., Makni Ayadi, F., Elfeki, A., 2019. Antioxidant and hepatopreventive effects of Cassia angustifolia extract against carbon tetrachloride-induced hepatotoxicity in rats. Arch. Physiol. Biochem., 1–11

Blumenthal, M., Goldberg, A., Brinckmann, J., 2000. Herbal medicine. Expanded commission E monographs, Integrative Medicine Communications, Newton.

Campos, J.F., de Castro, D.T.H., Damião, M.J., Vieira Torquato, H. F., Paredes-Gamero, E.J., Carollo, C.A., Estevinho, L.M., de PicoliSouza, K., Santos, E.L.D., 2016. The Chemical profile of Senna velutina leaves and their antioxidant and cytotoxic effects. Oxid. Med. Cell. Longev., 8405957

Coelho, I., Castanheira, I., Ordado, J.M., Donard, O., Silva, J.A.L., 2017. Recent developments and trends in the application of strontium and its isotopes in biological related fields. TrAC-Trends Analyt. Chem. 90, 45–61.

Cristoforetti, G., Tognoni, E., Gizzi, L.A., 2013. Thermodynamic states in laser induced plasmas: from the general case to laser-induced breakdown spectroscopy plasmas. Spectrochim. Acta B 90, 1–22.

Cristoforetti, G., De Giacomo, A., Dell'Aglio, M., Legnaioli, S., Tognoni, E., Palleschi, V., Omenetto, N., 2010. Local thermodynamic equilibrium in laser-induced breakdown spectroscopy: beyond the McWhirter criterion. Spectrochim. Acta B 65 (1), 86–95.

Das, S., Choudhuri, D., 2020. Dietary calcium regulates the insulin sensitivity by altering the adipokine secretion in high fat diet induced obese rats. Life Sci. 117560.

Das, S., Choudhuri, D., 2019. Calcium supplementation shows a hepatoprotective effect against high-fat diet by regulating oxidative-induced inflammatory response and lipogenesis activity in male rats. J. Tradit. Complement. Med. 10 (5), 511–519.

da Silva Gomes, M., Junior, D.S., Nunes, L.C., De Carvalho, G.G.A., de Oliveira Leme, F., Krug, F.J., 2011. Evaluation of grinding methods for pellets preparation aiming at the analysis of plant materials by laser induced breakdown spectrometry. Talanta 85 (4), 1744–1750.

de Carvalho, G.G.A., Junior, D.S., Nunes, L.C., da Silva Gomes, M., de Oliveira Leme, F., Krug, F.J., 2012. Effects of laser focusing and fluence on the analysis of pellets of plant materials by laser-induced breakdown spectroscopy. Spectrochim. Acta B 74, 162–168.

de Nascimento, M.N.G., Martins, M.M., Cunha, L.C.S., de Souza Santos, P., Goulart, L.R., de Souza Silva, T., Martins, C.H.G., Morais, S.A.L., Pivatto, M., 2020. Antimicrobial and cytotoxic activities of Senna and Cassia species (Fabaceae) extracts. Ind. Crops Prod. 148, 11.

Eidi, A., Mortazavi, P., Moradi, F., Rohani, A.H., Safi, S., 2013. Magnesium attenuates carbon tetrachloride-induced hepatic injury in rats. Magnes. Res. 26 (4), 165–175.

El Sherbini, M., Al Aamer, A.A.S., 2012. Measurement of plasma parameters in laser-induced breakdown spectroscopy using Si-lines. WJNSE 2 (04), 206.

Farid, A., Kamel, D., Montaser, S.A., Ahmed, M.M., El Amir, M., El Amir, A., 2020. Synergetic role of senna and fennel extracts as antioxidant, anti-inflammatory and anti-mutagenic agents in irradiated human blood lymphocyte cultures. J. Radiat. Res. Appl. Sci. 13 (1), 191–199.

Gondal, M.A., Habibullah, Y.B., Oloore, L.E., Iqbal, M.A., 2015. Determination of carcinogenic fluorine in cigarettes using pulsed UV laser-induced breakdown spectroscopy. Appl. Opt. 54 (17), 5560–5567.

Gondal, M.A., Dastageer, M.A., Maslehuddin, M., Alnehmi, A.J., Al-Amoudi, O.S.B., 2012. Detection of sulfur in the reinforced concrete structures using a dual pulsed LIBS system. Opt. Laser Techn. 44, 566–571.

Guerrero-Romero, F., Simental-Mendía, L.E., Hernández-Ronquillo, G., Rodriguez-Morán, M., 2015. Oral magnesium supplementation improves glycaemic status in subjects with prediabetes and hypomagnesaemia: a double-blind placebo-controlled randomized trial. Diabetes Metab. 41 (3), 202–207.

Hanif, M.A., Nawaz, H., Khan, M.M., Byrne, H.J., 2020. Medicinal Plants of South Asia: Novel Sources for Drug Discovery. Elsevier Ltd..

Harilal, S.S., Bindhu, C.V., Issac, R.C., Nampoori, V.P.N., Vallabhan, C.P.G., 1997. Electron density and temperature measurements in a laser produced carbon plasma. J. Appl. Phys. 82 (5), 2140–2146.

Hegazy, H., Abdel-Wahab, E.A., Abdel-Rahim, F.M., Allam, S.H., Abd ElDaim, M.A., 2014. Evaluation of plasma produced by first and second harmonic nano-second laser for enhancing the capability of laser induced breakdown spectroscopy technique. Eur. Phys. J. D 68 (5), 107.

Hussain, T., Gondal, M.A., 2008. Detection of toxic metals in waste water from dairy products plant using laser induced breakdown spectroscopy. Bullet. Environ. Cont. Toxicol. 80, 561–565.

Inoue Andrade, F., Purgato, G.A., Faria Maia, T.D., Pais Siqueira, R., Lima, S., Diaz, G., Diaz, M.A.N., 2015. Chemical constituents and an alternative medicinal veterinary herbal soap made from Senna macranthera. Evid.-Based Complementary Altern. Med. 217598.

Jabbar, A., Akhtar, M., Mehmood, S., Kurniawan, K.H., Hedwig, R., Baig, M.A., 2019. Analytical approach of laser-induced breakdown spectroscopy to detect elemental profile of medicinal plants leaves. Indones. J. Chem. 19 (2), 430–440.

Jani, D.K., Goswami, S., 2020. Antidiabetic activity of Cassia angustifolia Vahl. and Raphanus sativus Linn. leaf extracts. J. Tradit. Complement. Med. 10 (2), 124.

Kamaraj, C., Rahuman, A.A., Mahapatra, A., Bagavan, A., Elango, G., 2010. Insecticidal and larvicidal activities of medicinal plant extracts against mosquitoes. Parasitol. Res. 107 (6), 1337–1349.

Khaliq, H., Juming, Z., Ke-Mei, P., 2018. The physiological role of boron on health. Biol. Trace Elem. Res. 186 (1), 31–51.

Khan, F.A., Akhtar, S., Almohazey, D., Alomari, M., Almofty, S.A., Badr, I., Elaissari, A., 2019. Targeted delivery of poly (methyl methacrylate) particles in colon cancer cells selectively attenuates cancer cell proliferation. Artif. Cells Nanomed. Biotechnol. 47 (1), 1533–1542.

Khan, F.A., Akhtar, S., Almohazey, D., Alomari, M., Almofty, S.A., Eliassari, A., 2018a. Fluorescent magnetic submicronic polymer (FMSP) nanoparticles induce cell death in human colorectal carcinoma cells. Artif. Cells Nanomed. Biotechnol. 46 (sup3), S247–S253.

Khan, F.A., Akhtar, S., Almohazey, D., Alomari, M., Almofty, S.A., 2018b. Extracts of clove (syzygium aromaticum) potentiate FMSP-nanoparticles induced cell death in MCF-7 cells. Int. J. Biomater., 8479439

Kravchenko, J., Darrah, T.H., Miller, R.K., Lyerly, H.K., Vengosh, A., 2014. A review of the health impacts of barium from natural and anthropogenic exposure. Environ. Geochem. Health 36 (4), 797–814.

Levine, K.E., Ross, G.T., Fernando, R.A., Blake, J.C., Sparacino, C. M., Pellizzari, E.D., 2004. Trace element content of senna study material and selected senna-based dietary supplements as determined by inductively coupled plasma-optical emission spectrometry and inductively coupled plasma-mass spectrometry. Commun. Soil Sci. Plant Anal. 35 (5–6), 835–851.

Li, Y., Zhang, H., Jiang, Z., Li, Z., Hu, C., 2014. Spectroscopic characterization of aluminum plasma using laser-induced breakdown spectroscopy. Optik 125 (12), 2851–2855.

Liu, X., Zhang, Q., Wu, Z., Shi, X., Zhao, N., Qiao, Y., 2015. Rapid elemental analysis and provenance study of Blumea balsamifera DC using laser-induced breakdown spectroscopy. Sensors 15 (1), 642–655.

Mehder, O., Gondal, M.A., Dastageer, M.A., Habibullah, Y.B., Iqbal, M.A., Oloore, L.E., Gondal, B., 2016. Direct spectral analysis and determination of high content of carcinogenic bromine in bread using UV pulsed laser induced breakdown spectroscopy. J. Environ. Sci. Health B 51 (6), 358–365.

Mehta, S., Rai, P.K., Rai, N.K., Rai, A.K., Bicanic, D., Watal, G., 2011. Role of spectral studies in detection of antibacterial phytoelements and phytochemicals of Moringa oleifera. Food Biophys. 6 (4), 497–502.

Nielsen, F.H., 2014. Update on human health effects of boron. J. Trace Elem. Med. Biol. 28 (4), 383–387.

Nordberg, G.F., Fowler, B.A., Nordberg, M., 2014. Handbook on the Toxicology of Metals. Academic press, London.

Osman, N.N., Jambi, E.J., Aseri, N.H., 2017. Assessment of antidiabetic and antioxidant activities of Cassia angustifolia and Feoniculum vulgare in diabetic rats. Int. J. Pharm. Res. Allied Sci. 6 (2), 149–162.

Pilmane, M., Salma-Ancane, K., Loca, D., Locs, J., Berzina-Cimdina, L., 2017. Strontium and strontium ranelate: Historical review of some of their functions. Mater. Sci. Eng. C 78, 1222–1230.

Rehan, I., Gondal, M.A., Almessiere, M.A., Dakheel, R.A., Rehan, K., Sultana, S., Dastageer, M.A., 2021. Nutritional and toxic elemental analysis of dry fruits using laser induced breakdown spectroscopy (LIBS) and inductively coupled plasma atomic emission spectrometry (ICP-AES). Saudi J. Biol. Sci. 28 (1), 408–416.

Rehan, I., Gondal, M.A., Rehan, K., Sultana, S., Dastageer, M.A., Al-Adel, F.F., 2019. LIBS for the detection of lead in ready to use henna paste and nutrients in fresh henna leaves and cultivated soils. Talanta 199, 203–211.

Rehman, S., Asiri, S.M., Khan, F.A., Jermy, B.R., Khan, H., Akhtar, S., Al-Jindan, R., Khan, K.M., Qurashi, A., 2019. Biocompatible tin oxide nanoparticles: synthesis, antibacterial, anticandidal and cytotoxic activities. ChemistrySelect 4 (14), 4013–4017.

Ritsema, G.H., Eilers, G., 1994. Potassium supplements prevent serious hypokalaemia in colon cleansing. Clin. Radiol. 49 (12), 874–876.

Rodríguez-Morán, M., Guerrero-Romero, F., 2003. Oral magnesium supplementation improves insulin sensitivity and metabolic control in type 2 diabetic subjects: a randomized double-blind controlled trial. Diabetes Care 26 (4), 1147–1152.

Sarkar, A., Singh, M., 2017. Laser-induced plasma electron number density: Stark broadening method versus the Saha-Boltzmann equation. Plasma Sci. Technol. 19, 025403.

Scio, E., Mendes, R.F., Motta, E.V., Bellozi, P.M., Aragão, D.M., Mello, J., Fabri, R.L., Moreira, J.R., de Assis, I.V.L., Bouzada, M. L.M., 2012. Antimicrobial and antioxidant activities of some plant extracts. In: Rao, V. (Ed.), Phytochemicals as Nutraceuticals-Global Approaches to Their Role in Nutrition and Health. Intech, Rijeka, pp. 21–42.

Senesi, G.S., Cabral, J., Menegatti, C.R., Marangoni, B., Nicolodelli, G., 2019. Recent advances and future trends in LIBS applications to agricultural materials and their food derivatives: an overview of developments in the last decade (2010–2019). Part II. Crop plants and their food derivatives. TrAC. Trend. Anal. Chem. 118, 453–469.

Shaikh, N.M., Hafeez, S., Rashid, B., Baig, M.A., 2007. Spectroscopic studies of laser induced aluminum plasma using fundamental, second and third harmonics of a Nd: YAG laser. Eur. Phys. J. D 44 (2), 371–379.

Sigel, A., Sigel, H., Sigel, R.K., 2013. Interrelations Between Essential Metal Ions and Human Diseases. Springer, Dordrecht.

Silva, C.R., Monteiro, M.R., Rocha, M.R., Ribeiro, A.F., Caldeira-de-Araujo, A., Leitão, A.C., Bezerra, R.J.A.C., Pádula, M., 2008. Assessment of antimutagenic and genotoxic potential of senna (Cassia angustifolia Vahl.) aqueous extract using in vitro assays. Toxicol. In Vitro 22 (1), 212–218.

Tognoni, E., Cristoforetti, G., Legnaioli, S., Palleschi, V., Salvetti, A., Müller, M., Panne, U., Gornushkin, I., 2007. A numerical study of expected accuracy and precision in calibration free laser-induced breakdown spectroscopy in the assumption of ideal analytical plasma. Spectrochim. Acta B 62 (12), 1287–1302.

Tripathi, Y.C., 1999. Cassia angustifolia, a versatile medicinal crop. Int. Tree Crops J. 10 (2), 121–129.

Tripathi, D.K., Pathak, A.K., Chauhan, D.K., Dubey, N.K., Rai, A. K., Prasad, R., 2015. An efficient approach of laser induced breakdown spectroscopy (LIBS) and ICAP-AES to detect the elemental profile of Ocimum L. species. Biocatal. Agric. Biotechnol. 4 (4), 471–479.

Trumbo, P., Yates, A.A., Schlicker, S., Poos, M., 2001. Dietary reference intakes: vitamin A, vitamin K, arsenic, boron, chromium, copper, iodine, iron, manganese, molybdenum, nickel, silicon, vanadium, and zinc. J. Acad. Nutr. Diet. 101 (3), 294.

Uluisik, I., Karakaya, H.C., Koc, A., 2018. The importance of boron in biological systems. J. Trace Elem. Med. Biol. 45, 156–162.

Usmanghani, K., Saeed, A., Alam, M.T., 1997. Indusyunic Medicine: Traditional Medicine of Herbal, Animal, And Mineral Origin in Pakistan. Dept. of Pharmacognosy Faculty of Pharmacy, University of Karachi, Karachi.

VijayaSekhar, V.E., Prasad, M.S., Joshi, D.S., Narendra, K., Satya, A. K., Rao, K.S.S., 2016. Assessment of phytochemical evaluation and in-vitro antimicrobial activity of Cassia angustifolia. Int. J. Pharmacogn. Phytochem. Res. 8 (2), 305–312.

Vincent, J.B., 2003. The potential value and toxicity of chromium picolinate as a nutritional supplement, weight loss agent and muscle development agent. Sports Med. 33 (3), 213–230.

Viswanathan, S., Nallamuthu, T., 2012. Phytochemical screening and antimicrobial activity of leaf extracts of Senna alexandrina Mill. against human pathogens. IJCS 2, 51–56.

Vitalone, A., Di Giacomo, S., Di Sotto, A., Franchitto, A., Mammola, C.L., Mariani, P., Mastrangelo, S., Mazzanti, G., 2011. Cassia angustifolia extract is not hepatotoxic in an in vitro and in vivo study. Pharmacology 88 (5–6), 252–259.

Willhite, C.C., Karyakina, N.A., Yokel, R.A., Yenugadhati, N., Wisniewski, T.M., Arnold, I.M., Krewski, D., 2014. Systematic review of potential health risks posed by pharmaceutical, occupational and consumer exposures to metallic and nanoscale aluminum, aluminum oxides, aluminum hydroxide and its soluble salts. Crit. Rev. Toxicol. 44 (sup4), 1–80.

Zhu, C., Tang, Z., Li, Q., Zhou, R., Lv, J., Zhang, W., Zhan, K., Li, X., Zeng, X., 2020. Lead of detection in rhododendron leaves using laser-induced breakdown spectroscopy assisted by laser-induced fluorescence. Sci. Total Environ. 738, 139402.